DOI 10.1515/ama-2017-0010

ANALYSIS OF FORCE IN MR FLUIDS DURING OSCILLATORY COMPRESSION SQUEEZE

Wojciech HORAK[*], Bogdan SAPIŃSKI[**], Marcin SZCZĘCH[*]

[*]AGH University of Science and Technology Faculty of Mechanical Engineering and Robotics, Department Department of Machine Design and Technology, al. Mickiewicza 30, 30-059 Kraków, Poland
[**]AGH University of Science and Technology, Faculty of Mechanical Engineering and Robotics, Department of Process Control, al. Mickiewicza 30, 30-059 Kraków, Poland

horak@agh.edu.pl, deep@agh.edu.pl, szczech@agh.edu

received 19 April 2016, revised 10 March 2017, accepted 13 March 2017

Abstract: This study investigates the behaviour of MR fluids in the oscillatory compression squeeze mode. Experiments were performed on commercially available MR fluids in the purpose-built experimental set-up. The influence of MR fluid's properties and magnetic flux density on the force generated during the squeeze mode was investigated.

Key words: Mr Fluid, Oscillatory Squeeze Mode, Force, Experiment

1. INTRODUCTION

Magnetorheological (MR) fluids are categorised as smart materials whose properties vary under the influence of external magnetic fields. MR fluids contain ferromagnetic particles 0.1 to 10 μm in diameter suspended in a carrier fluid. In most engineering applications the carrier fluid is a mineral or synthetic oil. Additionally MR fluid particles are covered with a surfactant to enhance the sediment stability and to prevent particle aggregation.

In the absence of magnetic field MR fluids display rheological properties that are typical of non-homogeneous suspensions. In the presence of magnetic field, the structure of MR fluid gets changed and its rheological characteristics will change as well (Wang and Liao, 2011; Zubieta et al., 2009).

The direction of the fluid flow and that of magnetic field action are interrelated, hence several modes of MR fluid operation can be distinguished: the flowing mode, the sheer mode, squeeze mode and the gradient pinch mode (Gołdasz and Sapiński, 2015). So far only the flow-mode and shear-mode devices have been successfully commercialised. To the author's best knowledge, there are few studies exploring the behaviour of MR fluids in the squeeze mode and the involved phenomena (Farjoud et al., 2009; 2011; Chaoyang et al., 2013; Kuzhir et al., 2008; Mazlan et al., 2007). Moreover, no hardware handling the squeeze mode operation has been reported beyond the academia so far, with just one exception (Kim, 2014).

In the squeeze mode the working gap height varies in the direction parallel to that of the magnetic field. As the distance between the opposing surfaces changes, the fluid is squeezed out. The model of MR fluid behaviour in the squeeze mode is shown in Fig. 1. In the absence of magnetic field, the magnetic moments of particles have haphazard directions and the fluid will not exhibit any magnetic properties. In the presence of magnetic field and at the constant gap height h, magnetic moments of particles are arranged along the magnetic field lines H. That happens as a result of particles' rotating in the carrier fluid (Brownian mechanism) or due to the moment being rotated within the particle structure (Neel mechanism) (Kuzhir et al., 2008). Particles in the carrier fluid are arranged in column-like structures. When squeezed (displacement Δh, see Fig. 1c) the structures get deformed whilst their thickness are increased (Horak, 2013; Tao, 2001). Thus MR fluid provides increased resistance to compressive loading and its yield stress tends to increase (Sapiński and Szczęch, 2013; Tao, 2011).

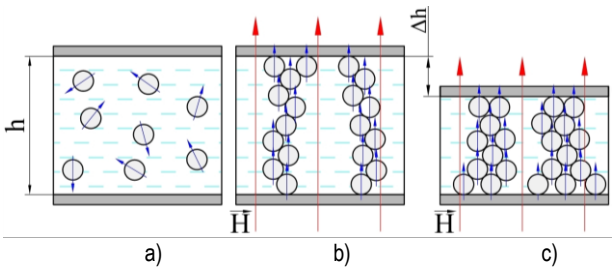

Fig. 1. MR fluid behaviour: a) in the absence of magnetic field; b) under magnetic field; c) in squeeze mode

In the oscillatory compression squeeze mode, MR fluids may tend to exhibit the clumping behaviour (Farjoud et al., 2008; 2011), and the carrier fluid between the particles tends to precipitate (Sapiński et al., 2014). The clumping behaviour consists in particles' being aggregated. In the case of fluid precipitation beyond the squeeze zone, the particles are retained in the zone exposed to magnetic field. Both effects are manifested in the macro scale by an increase in the squeeze resistance in the repeated load cycles.

Due to complexity of phenomena involved in the squeeze mode the analysis of this mode of MR fluid operation is fraught with difficulties. No mathematical model has been developed yet providing a comprehensive description of the MR fluid behaviour in the squeeze mode. There are two distinct approaches to the

DOI 10.1515/ama-2017-0010

modelling of MR fluid behaviour in the squeeze mode: that associated with the quasi-static input (Farjoud et al., 2008; Horak, 2013; Sapiński et al., 2013) and dynamic input (Chen et al., 2016).

The parameter that is of primary importance in investigations of the MR fluid behaviour in the squeeze mode is the compression force. Major determinants of this force include the volumetric fraction of particles, compression rate, magnetic flux density, particle shape and their magnetic properties (particularly the saturation magnetisation). Viscosity of the carrier fluid is of great importance too as it affects the resistance to the ferromagnetic particles' motion. Further, the presence of a surfactant covering the particles affects the magnitude of the friction force between the particles.

This study summarises the results of investigations of selected MR fluids during the oscillatory compression squeeze with the constant contact surface. No MR fluids are available on the market dedicated for squeeze mode operation exclusively, hence the testing was done on samples of MR fluids recommended by manufacturers for use in vibration dampers. This study is the continuation of the authors' research work (Sapiński et al., 2013). The purpose of the study was to find out how the force acting during the oscillatory quasi-static squeeze should vary in time. Furthermore, the behaviours of various MR fluids operated in that mode were compared and analysed.

2. INVESTIGATED FLUIDS

Testing was done on three MR fluids: Basonetic 2040, Basonetic 4035 and MRF-122EG. Basonetic fluids were manufactured by the BASF (http://www.basonetic.com/) company and MRF-122EG by the LORD Corporation (http://www.lord.com/). Properties of those fluids are compiled in Tab. 1.

Tab. 1. Properties of investigated MR fluids

No	MR fluid	Density	Dynamic viscosity B=0 mT, $\dot{\gamma}$=100 1/s, t=25°C	Saturation magnetization
		g/cm^3	mPa·s	kA/m
1	Basonetic 4035	2.68	106	417
2	Basonetic 2040	2.47	956	418
3	MRF-122EG	2.38	127	359

MR fluids Basonetic 4035 and MRF-122EG have a similar zero-field dynamic viscosity (indicating the similar viscosity of the carrier fluid) but differ significantly in the level of saturation magnetisation. Basonetic 4035 and Basonetic 2040 display a similar level of saturation magnetisation, however, Basonetic 2040 features a higher dynamic viscosity than Basonetic 4035.

3. EXPERIMENTAL SET-UP

Tests were performed in the experimental set-up described in Salwiński et al. (2014). Device and incorporating a test cell, and shown schematically in Fig. 2. The key component is a frame (Fig. 2a) supporting a linear servo motor 1 enabling the position of the measuring plate to be altered with the accuracy of 1 μm. A force sensor 2 is attached to the motor, used for measuring the tensile and compression forces. The sample of the MR fluid was placed inside the test cell 3.

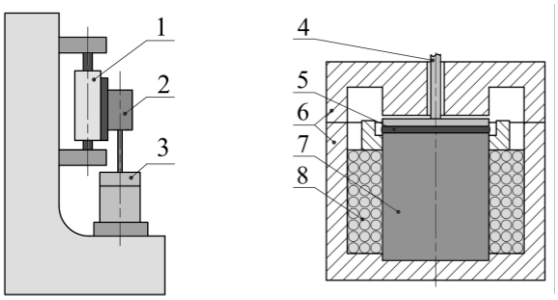

Fig. 2. Schematic diagram: a) experimental set-up; b) test cell

The investigated sample of MR fluid 5 was placed between the electromagnet cores 7 and a mobile plate made of a paramagnetic material 4. The magnetic circuit is closed by the cell housing 6. The magnetic flux density is altered by varying the current intensity in the electromagnet coil 8. Grooves are provided in the electromagnet core and in the housing to allow the flow of the cooling agent, which ensures the temperature stabilisation of the system. All experiments were conducted at the temperature 25°C. A PC with the dedicated software LabView enables the control of position and speed of the linear motor and steering of the electromagnet power supply, as well as data acquisition.

The test geometry is shown in Fig. 3. A mobile plate with the diameter 45 mm was placed between the electromagnet core and the cell housing, having identical diameter. The height of the gap between the core 7 and the cover 6 is g=10 mm. The initial height of the gap is h_0= 1 mm, and the volume of sample V_s=1.6 ml. The maximal plate displacement during compression is Δh=0.2 mm.

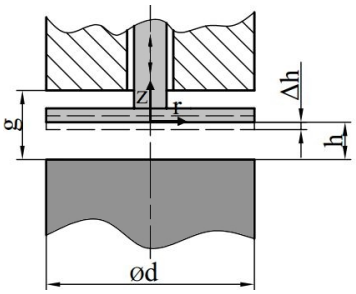

Fig. 3. Schematic of test geometry

Experiments were performed in the presence of the magnetic field with the flux density B: 70, 100, 140, 200 and 270 mT. The kinematic input was applied through the control of plate displacement Δh. The displacement pattern was taken to be trapezoidal, with the frequency f=0.1 Hz, corresponding to the velocity of the plate motion v= 0.04 mm/s. In accordance with the reference system (Fig. 3) the compressing force registered during the squeeze is assumed to have the negative sign.

4. RESULTS

In order to directly compared the plots of force registered at varied levels of magnetic flux density, the measurement data had to be corrected accordingly. For the given value of flux density, the constant force component was determined, expressed as the force acting when the plate was in its initial position (Δh=0 mm). The result correction consisted in subtracting thus deter-

DOI 10.1515/ama-2017-0010

mined constant component from the force registered in time.

The constant force components values are summarised in Fig. 4. Higher values are registered for MR fluids that exhibit higher saturation magnetisation. This issue is described in more detail elsewhere (Horak, 2013; Salwiński and Horak, 2012).

Fig. 5 summarises force measurement data for Basonetic 4035, corrected accordingly. Variations of the plate positions Δh are indicated on the plot. After correction, the measured force becomes F=0 N for t=0 s, regardless of the actual value of flux density.

For clarity, the force variation cycle is divided into 5 intervals (Fig. 5): A-B- compression squeeze; B-C- the mobile plate being stopped in its bottommost position Δh=0.2 mm (fluid being maximally compressed); C-D- returning to the plate's initial position. This interval is further sub-divided into: C-F0- time interval between the onset of the plate's upward movement and the instant the force value becomes zero for at least one of the fluids (the mobile plate moves and the gap becomes larger), F0-D- the time required for the plate to return to its initial position Δh=0 mm. The last interval D-A'- the plate being stopped in its initial position. Starting from the point A', the squeezing cycle is repeated.

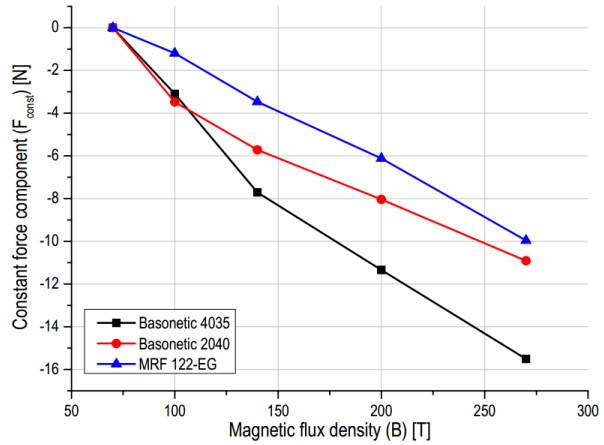

Fig. 4. Constant force component vs magnetic flux density

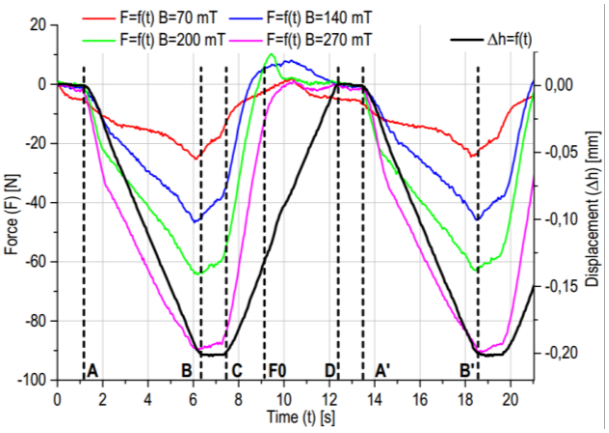

Fig. 5. Selected force plots (Basonetic 4035)

To adequately describe the force variability range in particular intervals, the force gradient value was determined expressed as the slope of the linear function approximating the force variability pattern.

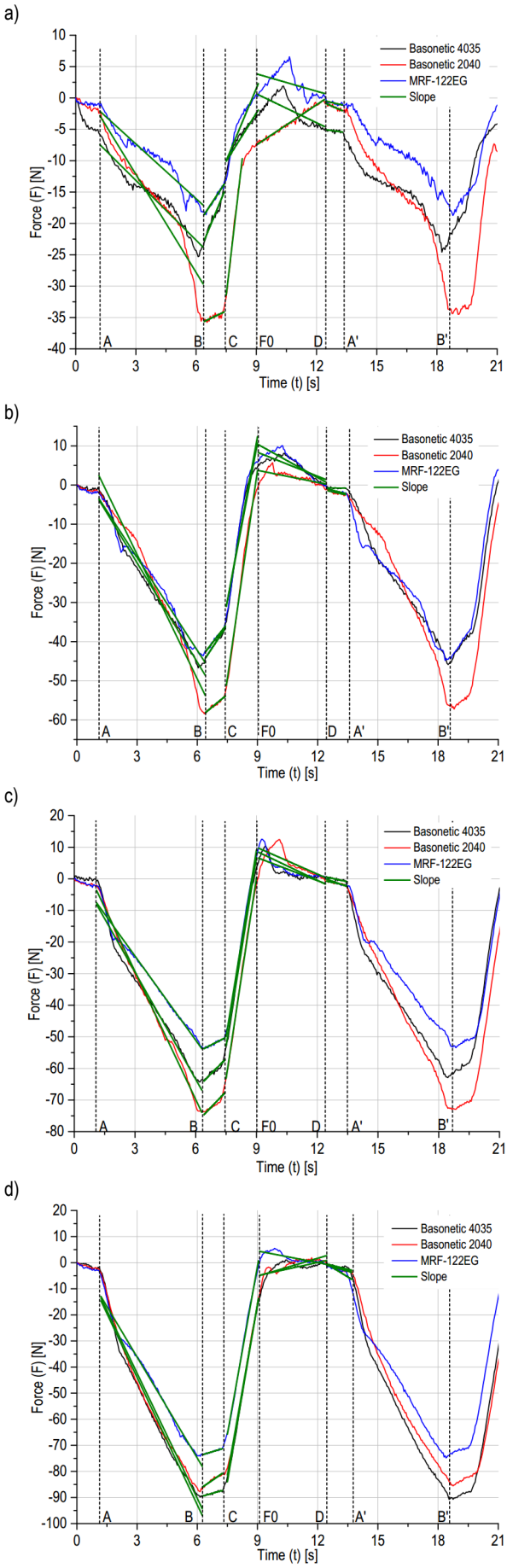

Fig. 6. Force vs time: a) 70 mT; b) 140 mT; c) 200 mT; d) 270 mT

DOI 10.1515/ama-2017-0010

Plots of force registered in particular intervals and the indicated sections of approximating linear functions are shown in Fig. 6a-d. Graphic representation of the slope values is given in Fig. 7.
During the compression squeeze (interval A-B) the compressing force increases nonlinearly (Fig. 6). The highest value of the force gradient for all magnetic flux density levels is registered for the fluid Basonetic 2040. Similar to Basonetic 4035, this fluid features the high saturation magnetisation, yet unlike Basonetic 4035, its zero field viscosity is much higher. For the flux density B=270 mT a slightly higher force gradient is registered for the fluid having a similar saturation magnetisation yet featuring a lower zero-field viscosity- Basonetic 4035 (Fig. 7d).

In the time interval corresponding to the plate being stopped in its bottommost position (B-C) and at the lowest level of magnetic flux density, the smallest force gradient is registered for Basonetic 2040.

a)

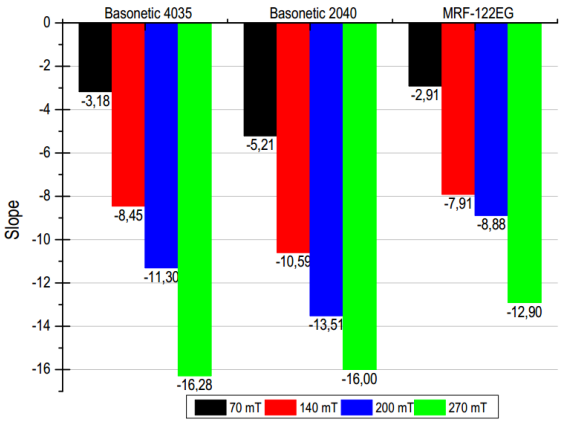

b)

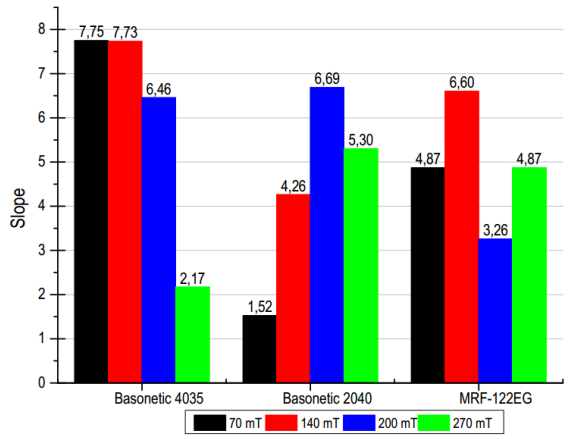

c)

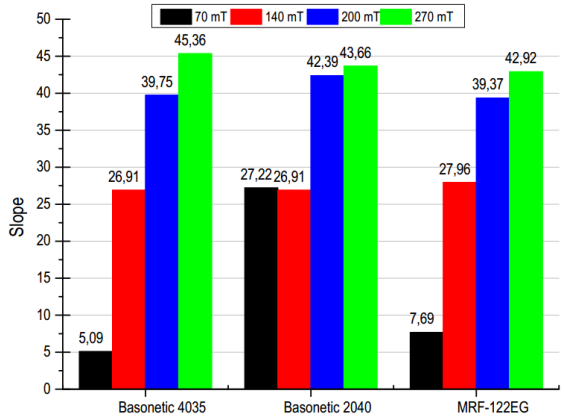

d)

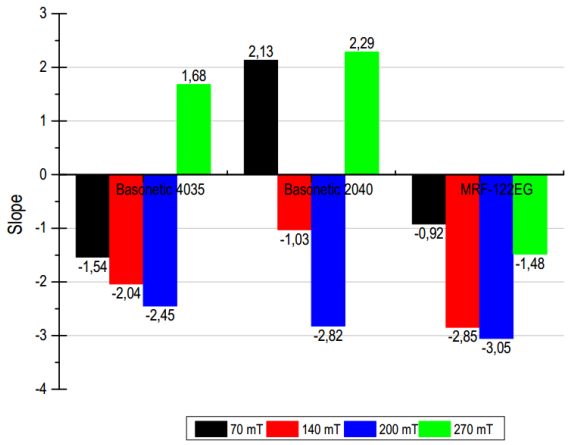

e)

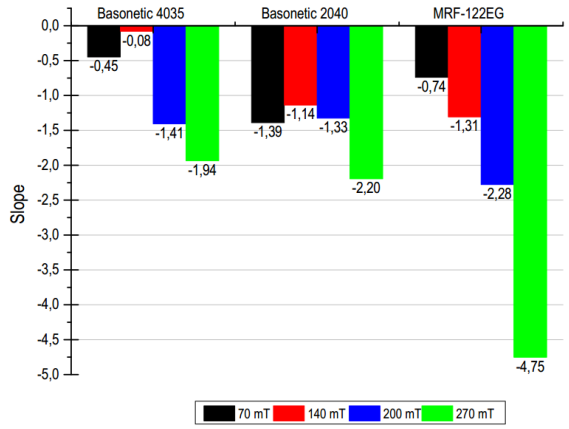

Fig. 7. Slope of force plots in the ranges: a) A-B; b)B-C; c) C-F0; d) F0-D; e) D-A'

When the magnetic flux density is the highest, the smallest gradient of force is registered for Basonetic 4035 (Fig. 7b). It is worthwhile to mention that the force gradient in the interval B-C ranges from 1.5 to more than 7.5 N/s, which implies force reduction by as much as 10% of its maximal value per second.

The gradient of compressing force during the phase when the plate moves upwards to its initial position (C-F0) is significantly higher than the force increase during compression squeeze. The higher the magnetic flux density, the greater this difference in force (Fig. 7 a, c).

The force pattern registered in the interval F0-D is the most complex. Whilst the plate moves upwards, the tensile force arises (the positive sense of the force vector) whose magnitude will then decrease (Fig. 6a-d).

One has to bear in mind that interpolating the force plot in this interval with a straight line section leads to a major simplification, yet giving us an insight into a general trend of force variations.

At flux density B=140 and 200 mT all investigated fluids would exhibit a similar pattern of force variability. In the interval F0-D (Fig. 6b,d) there is a decrease in the tensile force. The higher the magnetic flux density, the greater the force gradient (Fig. 7d).

The experiment performed at the lowest flux density level (B=70 mT) revealed that in the entire sample tension interval, the value of the compressing force in the fluid of highest initial viscosity (Basonetic 2040) would decrease (Fig 6a).

During the experiments taken at B=270 mT the compressing force decreased for the two Basonetic fluids whilst for MRF-122EG it was the tensile force that decreased.

DOI 10.1515/ama-2017-0010

In the interval D-A' the compressing force increased for all investigated fluids. The higher the magnetic flux density, the faster the rate of force increase (Fig 7e).

5. CONCLUSIONS

To a certain extent, the changes of force measured in all investigated cases follow a similar pattern. In the first interval (A-B) there is a nonlinear increase of the compressing force. The highest gradient of the compressing force is registered for the fluid featuring the highest saturation magnetisation and highest zero-field viscosity (Basonetic 2040). An exception is the measurement taken at 270 mT, in this case the highest value is registered for Basonetic 4035.

When the plate is retained in its bottommost position (interval B-C), the compressing force will decrease in all investigated cases. In the case of fluid displaying low zero-field viscosity and high magnetisation (Basonetic 4035) decrease of the force value was more intensive for lower magnetic field strength through a reverse trend is revealed in the case of Basonetic 2040 which has a similar saturation magnetisation but is based on a high-viscosity carrier fluid (Fig. 6a).

During the return motion of the plate (C-D), the compressing force falls rapidly in the first phase (C-F0). For the investigated fluids, the compressing force during the return movement of the plate changes 2 or 3 times faster than the force increase during the squeeze. The higher the magnetic flux density, the faster the force decrease proceeds (Fig. 7c). In all cases considered in the study, during the further stage of the return motion (F0-D), the tensile force will arise and its value tends to decrease while the plate is approaching its initial position. This force can be partly caused by the fluid being sucked back, due to negative pressure produced during the upward movement. Most probably this force is also attributed to the fluid moving in the radial direction with respect to the plate axis during the tensile phase whilst the field gradient in the area of MR fluid application causes the fluid to move beyond the compression zone, due to the presence of an opening in the upper chamber.

In the last interval (D-A'), the compressing force increases when the plate is stopped in its initial position. The higher the magnetic flux density, the faster the force increase (Fig. 7e). The force which pushes the plates away from one another may be attributed to rebuild of column-like structures of particles contained in MR fluids.

REFERENCES

1. **Chaoyang G., Xinglong G., Shouhu X., Lijun Q., Qifan Y.** (2013), Compression behaviors of magnetorheological fluids under nonuniform magnetic field, *Rheologica Acta*, 52(2), 165–176.
2. **Chen, Peng and Bai, Xian-Xu and Qian, Li-Jun** (2016), Magnetorheological fluid behavior in high-frequency oscillatory squeeze mode: Experimental tests and modelling, *Journal of Applied Physics*, 119, 105101.
3. **Farjoud A., Cavey R., Ahmadian M., Craft M.** (2009) Magneto-rheological fluid behaviour in squeeze mode, *Smart Materials and Structures*, 18, 095001.
4. **Farjoud A., Craft M., Burke W., Ahmadian M.** (2011), Experimental investigation of MR squeeze mounts, *Journal of Intelligent Material Systems and Structures*, 22, 1645–1652.
5. **Farjoud A., Vahdati N., Fah Y.** (2008), MR-fluid yield surface determination in disc-type MR rotary brakes, *Smart Materials and Structures*, 17(3), 1-8.
6. **Gołdasz J., Sapiński B.** (2015), *Insight into Magnetorheological Shock Absorbers*, Springer International Publishing, Switzerland.
7. **Horak W.** (2013), *Theoretical and experimental analysis of magnetorheological fluid squeeze flow*, PhD Thesis (in Polish), AGH University of science and Technology, Krakow.
8. **Kim J. H.** (2014), *Damping force control filled with magnetorheological fluids and engine mount having the same*, US Patent, No. US 8,672,105 B2.
9. **Kuzhir P., Lopez-Lopez M. T., Vertelov G., Pradille Ch., Bossis G.** (2008), Oscillatory squeeze flow of suspensions of magnetic polymerized chains, *Journal of Physics: Condensed Matter*, 20(1), 1-5.
10. **López-López M.T, Kuzhir P**., et al. (2011), Normal stresses in a shear flow of magnetorheological suspensions: viscoelastic versus Maxwell stresses, *Journal of Rheology*, 54, 1119.
11. **Mazlan S. A., Ekreem, N.B., Olabi A.G.,** (2007) The performance of magnetorheological fluid in squeeze mode, *Smart Mater. Struct.*,16 1678–1682.
12. **Odenbach S., Pop L. M., Zubarev A. Yu**. (2007), Rheological properties of magnetic fluids and their microstructural background, GAMM-Mitteilungen, 30(1), 195-204.
13. **Salwiński J., Horak W**. (2012), Measurement of Normal Force in Magnetorheological and Ferrofluid Lubricated Bearings, *Key Engineering Materials*, 490, 25-32.
14. **Salwiński J., Horak W., Szczęch M.** (2014), Experimental apparatus for examination of magnetic fluid lubricated thrust bearing, *Scientific Papers of Silesian University of Technology*, 83, 243-249.
15. **Sapiński B., Horak W. Sioma A.** (2014), Experiments of MR fluid behaviour in the squeeze mode using the vision method, *Control Conference (ICCC), 15th International Carpathian*, Velke Karlovice, 513–516.
16. **Sapiński B., Horak W. Szczęch M.** (2013), Investigation of MR fluids in the oscillatory squeeze mode, *Acta Mechanica et Automatica*, 7(2), 111-116.
17. **Sapiński B., Szczęch M.** (2013), CFD model of a magnetorheological fluid in squeeze mode, *Acta Mechanica et Automatica*, 7(3), 180-183.
18. **Tao R.** (2001), Super-strong magnetorheological fluids, *Journal of Physics: Condensed Matter*, 13(50), 979–999.
19. **Wang, D.H., Liao, W.H**. (2011), Magnetorheological fluid dampers: a review of parametric modelling, *Smart Mater. Struct.*, 20, 023001.
20. **Zubieta M., Eceolaza S., Elejabarrieta M.J., Bou-Ali M. M.** (2009) Magnetorheological fluids: characterization and modeling of magnetization, *Smart Mater. Struct.*, 18, 095019.
21. BASF The Chemical Company, http://www.basonetic.com/.
22. LORD Corporation, http://www.lord.com/.

Acknowledgement: This work is supported by AGH University of Science and Technology under research program No. 11.11.130.958.